An efficient algorithm for simulation of forced deformable bodies interacting with incompressible flows; Application to fish swimming

Patrick Bontoux, Stéphane Viazzo, Kai Schneider, Seyed Amin Ghaffari

11th World Congress on Computational Mechanics (WCCM XI)
5th European Conference on Computational Mechanics (ECCM V)
6th European Conference on Computational Fluid Dynamics (ECFD VI)
E. Oñate, J. Oliver and A. Huerta (Eds)

AN EFFICIENT ALGORITHM FOR SIMULATION OF FORCED DEFORMABLE BODIES INTERACTING WITH INCOMPRESSIBLE FLOWS; APPLICATION TO FISH SWIMMING

Patrick Bontoux[1], Stéphane Viazzo[2], Kai Schneider[3] and Seyed Amin Ghaffari[4]

[1] Professor, bontoux@L3M.univ-mrs.fr
[2] Professor, stephane.viazzo@L3M.univ-mrs.fr
[3] Professor, kschneid@cmi.univ-mrs.fr
[4] PhD student, corresponding author, ghaffari@L3M.univ-mrs.fr
Lab. M2P2-UMR 7340-CNRS, Aix-Marseille Université, Centrale Marseille, France

Key words: Fluid interaction with forced deformable bodies, Compact fourth-order direct Poisson solver, Volume penalization, Fish swimming/turning

Abstract. We present an efficient algorithm for simulation of deformable bodies interacting with two-dimensional incompressible flows. The temporal and spatial discretizations of the Navier-Stokes equations in vorticity stream-function formulation are based on classical fourth-order Runge-Kutta and compact finite differences. By using a uniform Cartesian grid we benefit from the advantage of a new fourth-order direct solver for the solution of the Poisson equation to ensure the incompressibility constraint down to machine zero. For introducing a deformable body in fluid flow, an immersed boundary method is applied to the solution of the Navier-Stokes equations as a forcing term. A Lagrangian structure grid with prescribed motion cover the deformable body interacting with surrounding fluid due to hydrodynamic forces and moment calculated on an Eulerian reference Cartesian grid. An efficient law for curvature control of an anguilliform fish, swimming to a prescribed goal, is proposed. Validation of the developed method shows the efficiency and expected accuracy of the algorithm for fish-like swimming control and also for a variety of fluid/solid interaction problems.

1 INTRODUCTION

The quantification and simulation of the flow around biological swimmers is one of the challenges in fluid mechanics. At the same time bio-inspired design of swimming robots are in growth [10]. The costs of experimental studies lead the researchers to develop for efficient predictive numerical algorithms for the hydrodynamic analyses of fish swimming.

Difficulties of numerical simulations of fish-like swimming are due to different reasons; One problem is efficient quantification of the kinematics of different species which seems to be far from the proposed simple laws in different studies. However the main swimming mechanism in the majority of anguilliform fishes consists of a sinusoidal wave enveloped by a profile, created by the backbone of the fish which movies from head to tail. The tail beat creates a reverse Kármán street of vortices and will push the fish forward, leaving a momentumless wake back. Efficient simulation of the incompressible flows is also an important problem, because the propagation of the perturbations with the sound speed in all directions in the incompressible media will lead to an elliptic equation. Thus the efficiency of the elliptic solver is crucial in dealing with the incompressible flow solvers. The third bottleneck in numerical simulations of fish-like swimming is the coupling of fluid solver with deformable, moving and rotating bodies. To overcome this difficulty volume penalization method which belongs to immersed boundary method family will be is used for efficient simulation of the fluid/solid interaction. In the procedure of the solution to the incompressible Navier-Stokes equations an elliptic Poisson equation which is the most time consuming part of the algorithm will encountered frequently. Direct methods like diagonalization or iterative methods (e.g. multi-grid and Krylov subspace methods) can be used. With the use of high-order discretization iterative methods will be less attractive because their rate of convergence is slow. On the other hand in direct methods memory limitation is restrictive for simulations over fine grids. Therefore decoupling of the directions by FFT based methods is very advantageous, however this method will put some limitations in the boundary conditions. We are presenting a new fourth-order solver for the Poisson equation which is a combination of a compact finite difference with sine FFT. The main advantages of our method are fourth-order accuracy, efficiency, the possibility to parallelization and convergence down to zero machine. Other advantages and limitations of the proposed solver are discussed in the paper. In the present work we will focus on some numerical aspects of efficient turning laws which is less studied by other researchers. To this end the method of quaternions is adapted to backbone kinematics description. We are applying compact finite differences to the vorticity stream-function formulation of the Navier-Stokes equations including penalization term [11]. An efficient direct method is presented to the solution of the Poisson equation. The code is developed in FORTRAN and is accessible for all [18]. The paper is organized as follows. Fist our methodology including governing equations and kinematics of a fish like-swimming will be presented. Then validation of the algorithm will be done. Next the results for swimming fish looking for a food will be reported. Finally the results will be discussed and some guides for the future works will be addressed.

2 GOVERNING EQUATIONS

The governing equations of the incompressible flows are the Navier-Stokes equations. In two-dimensional problems the vorticity ω and stream-function ψ formulation is more efficient than primitive variables, see [1] and [2]. By taking the curl of the Navier-Stokes

equations, one obtains the vorticity transport equation:

$$\partial_t \omega + (\mathbf{u} \cdot \nabla)\omega = \nu \nabla^2 \omega + \nabla \times \mathbf{F} \ , \ \ \mathbf{x} \in \Omega \in \mathbb{R}^2 \tag{1}$$

where $\omega(\mathbf{x}, t) = \nabla \times \mathbf{u} = v_x - u_y$ denotes the vorticity, Ω is the spatial domain of interest, $\mathbf{u}(\mathbf{x}, t)$ is the velocity field, $\nu = \mu/\rho_f > 0$ is the kinematic viscosity of the fluid, ρ_f is the density and $\mathbf{F}(\mathbf{x}, t)$ is a source term. For a complete description of a particular problem, the above equations need to be complemented to describe an initial/boundary value problem (IBVP). The equation is parabolic in time and the velocity components are $(u, v) = (\partial_y \psi, -\partial_x \psi)$ with ψ being the stream-function, satisfying a Poisson equation

$$-\nabla^2 \psi = \omega \tag{2}$$

which is an elliptic equation in space. The penalization term for unit mass of the fluid reads,

$$\mathbf{F} = -\eta^{-1} \chi (\mathbf{u} - \mathbf{u}_P) \tag{3}$$

where $\mathbf{u}_P(\mathbf{x}, t)$ is the velocity field of the immersed body. The Navier-Stokes equations are written for unit mass of the fluid, therefore the dimension of the terms like $\mathbf{F}$ is acceleration, i.e., $[LT^{-2}]$. Penalization parameter η is the porosity (permeability) coefficient of the immersed body with dimension $[T]$. The mask (characteristic) function χ is dimensionless and describes the geometry of the immersed body.

$$\chi(\mathbf{x}, t) = \begin{cases} 1 & \mathbf{x} \in \Omega_b \\ 0 & \mathbf{x} \in \Omega_f \end{cases} \tag{4}$$

where Ω_f represents the domain of the flow and Ω_b represents the immersed body in the domain of the solution. The solution domain $\Omega = \Omega_f \cup \Omega_b$ is governed by the Navier-Stokes equations in the fluid regions and by Darcy's law in the penalized regions, when $\eta \to 0$. Classical fourth-order Runge-Kutta method [5] will be used for time integration of Eq. (1). All spatial derivatives will discretized with central explicit second-order or compact fourth-order finite difference methods [4]-[7]. For more details see [17].

2.1 Fourth-order fast Poisson solver

In the procedure of the solution to the incompressible Navier-Stokes equations an elliptic Poisson equation which is the most time consuming part of the algorithm is frequently encountered. The common case is the pressure Poisson equation frequently used with homogeneous Neumann boundary conditions, for the pressure correction in projection methods. Another example is in the vorticity stream-function formulation using equation (2) with Dirichlet boundary condition for vorticity and stream-function. Free slip ($\omega = 0$) boundary condition in a close rectangular domain ($\psi = 0$, all around) can cover all the test cases studied in present investigation. In the presence of periodic boundary conditions, FFT based direct solvers can be used to efficiently solve the Poisson equation with

high accuracy. Even if the flow is not periodic in all directions, like most of the practical problems, in accordance with the boundary conditions for elliptic equation (homogeneous Dirichlet/Neumann) *sine* or *cosine* FFT can be used. We are presenting a new direct fourth-order solver for the Poisson equation (2) which is a combination of a compact finite difference with sine FFT. The advantages of our method are fourth-order accuracy, compact tridiagonal stencil, possibility of extension to three dimension, less arithmetics, less memory usage in comparison to iterative methods and straightforward parallelization because of decoupling of the operations in different directions. Near linear strong scaling (speedup) and efficiency is reported by Laizet et al. in [12] for a similar direct solver. They introduced a dual domain decomposition (or pencil) method, in which information along a line is accessible for a CPU by alternative decomposition of domain in three directions. The limitations of our method (moreover the boundary conditions) is the use of uniform grid in the direction in which FFT is necessary. Usually when the solver of parabolic part is finite-difference, it is a custom to use a FDM discretization in one direction without lost of accuracy and efficiency (via direct tridiagonal solver), the advantage of this approach is the possibility of applying general boundary condition in that direction and using a refined mesh. The second-order version of this solver can be find in [6]. For a compact fourth-order collocated discretization of Poisson equation $-\nabla^2\psi = \omega$, over $N_x \times N_y$ grid points, by using Eq. (5)

$$\frac{\partial^2\psi}{\partial x^2} = \delta_x^2\psi - \frac{\Delta x^2}{12}\frac{\partial^4\psi}{\partial x^4} + O(\Delta x^4) \tag{5}$$

where δ_x^2 represents a central second-order estimation of the second derivative, for x direction we obtain

$$(\delta_x^2 - \frac{\Delta x^2}{12}\frac{\partial^4}{\partial x^4} + \partial_{yy})\psi = -\omega \tag{6}$$

because of the presence of Δx^2 factor behind fourth-order derivative, this term cannot be dropped and must be evaluated by second-order accuracy, therefor, the hole approximation scheme yield the fourth-order accuracy. Fourth-order derivative can be evaluated by using the original Poisson equation $-\nabla^2\psi = \omega$, and successive differentiating it with respect to x (i.e., $\partial_{xx}\partial_{xx}\psi = -\partial_{xx}\partial_{yy}\psi - \partial_{xx}\omega$) replacing ∂_{xx} by δ_x^2, we find

$$(\delta_x^2 + \frac{\Delta x^2}{12}\delta_x^2\partial_{yy} + \partial_{yy})\psi = -\omega - \frac{\Delta x^2}{12}\delta_x^2\omega \tag{7}$$

by applying Fourier transform in y direction over Eq. (7) and replacing second derivatives by $-k_y^2\hat{\psi}$ in Fourier space, we have

$$(\delta_x^2 - \frac{\Delta x^2}{12}\delta_x^2 k_y'^2 - k_y'^2)\hat{\psi} = -\hat{\omega} - \frac{\Delta x^2}{12}\delta_x^2\hat{\omega} \tag{8}$$

Usually the exact wavenumber will replace by modified wavenumber $k_y'^2$ which permits to evaluate the difference between the finite-difference and the spectral approximation of the

second derivative [6]. For a fourth-order explicit finite-difference discretization, analytical relation for the scaled modified wavenumber of second derivative is given in [4] as follows

$$k_y'^2 = \frac{1}{\Delta y^2}\left[\frac{8}{3}\Big(1-\cos(\frac{k_y\pi}{N_y})\Big) - \frac{1}{6}\Big(1-\cos(\frac{2k_y\pi}{N_y})\Big)\right] \tag{9}$$

The final tridiagonal system to be solved for the solution in Fourier space for each wavenumber of ψ in y direction is

$$\beta\hat{\psi}_{i+1,m} - (2\beta + k_y'^2)\hat{\psi}_{i,m} + \beta\hat{\psi}_{i-1,m} = -(\hat{\omega}_{i+1,m} + 10\hat{\omega}_{i,m} + \hat{\omega}_{i-1,m})/12 \tag{10}$$

for $i = 2, ..., N_x - 1$, where $\beta = \Delta x^{-2} - k_y'^2/12$. In summary, first a one-dimensional direct-FFT of the forcing function is performed in y direction, then for each line in x direction the tri-diagonal system (10) must be solved to find the solution ψ in wavenumber space, next inverse-FFT of the solution must be performed. For the real data with zero value at the boundaries (homogeneous Dirichlet boundary condition, i.e., $\psi = \omega = 0$), the natural Fourier transform to use is the *sine* transform, see [5]. The direction of FDM and FFT can be changed to consider no-slip boundary condition in y direction. For taking into account inflow/outflow boundary condition the mean flow must reduce from $\mathbf{u} = \mathbf{U}_\infty - \mathbf{U}$ in vorticity transport equation (1) to force $\psi = 0$ at the boundary. This is equivalent to move the grid with $\mathbf{U}_\infty$ and writing the Navier-Stokes equations in moving reference frame instead of Galilean inertial frame [13].

3 KINEMATICS OF THE FISH

The geometrically exact theory of nonlinear beams, is developed by Simo [3] and extended for fish vertebral by Boyer et al. [8]. In this theory, the beam is considered as a continuous assembly of rigid sections of infinitesimal thickness, i.e., a one-dimensional Cosserat medium. We are summarizing the exact kinematics of fish backbone in three dimensions for interested readers and future developments, but all the cases in this paper are limited to two-dimensions. Following Boyer et al. the kinematics of the backbone for Eel-like fishes can be determined by integration along arc-length ξ starting with head's situation as boundary condition. The variation of the orientation is obtained by

$$\frac{\partial Q}{\partial \xi} = \frac{1}{2}M(\Omega)Q \tag{11}$$

where $Q = (\cos\frac{\phi}{2}, a_x\sin\frac{\phi}{2}, a_y\sin\frac{\phi}{2}, a_z\sin\frac{\phi}{2})^T$ are unit normalized $(q_0^2+q_1^2+q_2^2+q_3^2)^{1/2} = 1$ quaternions that represent the head frame's orientation with respect to the inertial frame. $M(\Omega)$ is an anti-symmetric tensor,

$$M(\Omega) = \begin{bmatrix} 0 & -\omega_1 & -\omega_2 & -\omega_3 \\ \omega_1 & 0 & \omega_3 & -\omega_2 \\ \omega_2 & -\omega_3 & 0 & \omega_1 \\ \omega_3 & \omega_2 & -\omega_1 & 0 \end{bmatrix} \tag{12}$$

where $\Omega = (\omega_1, \omega_2, \omega_3)^T$ denotes the mean angular velocity. The geometry $R = (x, y, z)^T$ in Galilean reference frame is stated by

$$\frac{\partial R}{\partial \xi} = Rot(Q)K \tag{13}$$

where k_2 and k_3 in $K = (k_1, k_2, k_3)^T$ stand for the Eel's backbone transversal curvature and k_1 represent the rate of rotation (twist) of section around backbone along ξ direction. The rotation matrix in terms of the quaternions is given by

$$Rot = 2 \begin{bmatrix} q_0^2 + q_1^2 - \frac{1}{2} & q_1 q_2 - q_0 q_3 & q_1 q_3 + q_0 q_2 \\ q_1 q_2 + q_0 q_3 & q_0^2 + q_2^2 - \frac{1}{2} & q_2 q_3 - q_0 q_1 \\ q_1 q_3 - q_0 q_2 & q_2 q_3 + q_0 q_1 & q_0^2 + q_3^2 - \frac{1}{2} \end{bmatrix} \tag{14}$$

The variation of linear $V = (v_1, v_2, v_3)^T$ and angular $\Omega = (\omega_1, \omega_2, \omega_3)^T$ velocities in local frame, i.e., the frame attached to the body are given by

$$\frac{\partial}{\partial \xi} \begin{bmatrix} V \\ \Omega \end{bmatrix} = - \begin{bmatrix} K^\vee & \Gamma^\vee \\ 0 & K^\vee \end{bmatrix} \begin{bmatrix} V \\ \Omega \end{bmatrix} + \begin{bmatrix} \dot{\Gamma} \\ \dot{K} \end{bmatrix} \tag{15}$$

where $(.)$ represents time derivative, $(\vee)$ stands for anti-symmetric matrix constructed from a given vector, e.g.,

$$\Gamma^\vee = \begin{bmatrix} 0 & -\gamma_3 & \gamma_2 \\ \gamma_3 & 0 & -\gamma_1 \\ -\gamma_2 & \gamma_1 & 0 \end{bmatrix} \tag{16}$$

where $\Gamma = (\gamma_1, \gamma_2, \gamma_3)^T$ represents local transversal shearing whose first component is the rate of stretching. The accelerations can also deduced from time derivative of Eq. (15). For more details see [8], [10] and [16]. For finding the velocities in the frame attached to the head from velocities V_G in Galilean reference frame and inverse, we have

$$(v_1, v_2, v_3)^T = Rot^T (v_x, v_y, v_z)^T \tag{17}$$

By considering N $(1, ..., N_{points})$ discrete points on Eel's backbone, equations (11), (13) and (15) altogether must be integrated in space by a proper numerical method ($N_{eq} = 13$ in 3D). We are using fourth-order Runge-Kutta method for integration and comparison with first-order Euler method shows that RK4 can do better especially when the number of the points along the Eel's backbone is less than $N_{points} = 30$.

3.1 Fish in forward gait

Anguilliform swimming presented in Gazzola et al. [14] is considered for validation of the proposed algorithm. A periodic swimming law is defined by fitting the backbone of the fish to a given curve $y(x, t)$ keeping the backbone length l_{fish} fixed. Let ξ be the

arclength over curvilinear coordinate of the deformed backbone ($0 \leq \xi \leq l_{\text{fish}}$). For points uniformly distributed $\Delta\xi = l_{\text{fish}}/(N-1)$ over the backbone, y is given by

$$y(x,t) = a(x)\sin(2\pi(x/\lambda + ft)) \tag{18}$$

where λ is the wavelength, f is the frequency of the backbone and $a(x)$ is the envelope given by

$$a(x) = a_0 + a_1 x + a_2 x^2 \tag{19}$$

x is defined by inverting the arclength integral, i.e., $\Delta x = \Delta\xi/\sqrt{1+(\partial y/\partial x)^2}$. Wavelength of the fish is defined in accordance with the geometry of the backbone in Cartesian system. We need the curvature of the backbone to be able to use geometrically exact theory of nonlinear beams. One must switch from the Cartesian system to the curvature, thus second derivative of Eq. (18) will lead to

$$k(\xi,t) = (2a_2 - (2\pi/\lambda)^2 a(\xi))\sin(2\pi(\frac{\xi}{\lambda} + ft)) + (4\pi(a_1 + 2a_2\xi)/\lambda)\cos(2\pi(\frac{\xi}{\lambda} + ft)) \tag{20}$$

where $a(\xi) = a_0 + a_1\xi + a_2\xi^2$. The parameters used by Kern and Koumoutsakos [9] and Gazzola et al. [14] for the kinematics of the fish are as follows; $\lambda = 1$, $f = 1$, $a_2 = 0$, $a_1 = 0.125/(1+c)$, $a_0 = 0.125c/(1+c)$ and $c = 0.03125$. The buoyancy is equal to zero, i.e., $\rho_b = \rho_f$. The viscosity of the fluid is set to $\nu = 1.4 \times 10^{-4}$ resulting in a Reynolds number approximately $Re \approx 3800$, with an asymptotic mean velocity $U_{\text{forward}} \approx 0.52$. The simulations of Gazzola et al. [14] are carried out on a rectangular domain $(x,y) \in [0, 8l_{\text{fish}}] \times [0, 4l_{\text{fish}}]$ with resolution of 4096×2048 and penalization parameter $\eta = 10^{-4}$. We are performing our simulations on a rectangular domain $(x,y) \in [0, 10l_{\text{fish}}] \times [0, 5l_{\text{fish}}]$ by imposing penalization parameter inside the body equal to $\eta = 10^{-3}$ with resolution of 2049×1025 and 1025×513 and $\Delta t = 10^{-3}$. The centroid of the fish is initially positioned at $x_{\text{cg}} = 0.9L_x$ and $y_{\text{cg}} = 0.5L_y$ in our simulations. The forward velocities of the center of the mass computed with different methods/parameters are compared in Fig. 1. We impose two degree of liberty fixing the angular velocity equal to zero. The simulations start with the body and fluid at rest. The motion of the fish is initialized by gradually increasing the amplitude of the backbone through a sinusoidal function from zero to its designated value during the first period T in the reference simulations, i.e., [9] and [14], but we are not considering for this and starting by a sudden movement given by Eq. (18), therefore a deviation from the reference solution can be seen in the the first period. This deviation will continue systematically until the asymptotic velocity is reached at $t = 7$. The details of our algorithm is given in [17]. In our simulations a grid independent simulation is obtained with 2048×1025 grid points. The difference of two simulations with 2049×1025 and 1025×513 grid points can be seen in Fig. 1. Filtering of the hydrodynamics coefficients is necessary to prevent the simulation from divergence and non-physical results. We are using second-order exponential filtering instead of first-order filtering used in [9]. This process is like to adding a damper to the system therefore

a correct value for δ must be chosen for obtaining physical results via numerical tests. We propose values in the range of $\delta \in [0.01, 0.001]$ for fluid/solid interaction problems, however this can also depend to the manner of non-dimensionalization of the forces. In Fig. 1 the effect of filtering with two filter parameter, i.e., $\delta = 0.001$ and $\delta = 0.05$, can be seen. Filtering with a small filter parameter $\delta = 0.001$ will be more stable but instead will lead to smaller values in the terminal velocity and also smaller amplitude in its oscillations. See [17] for more details.

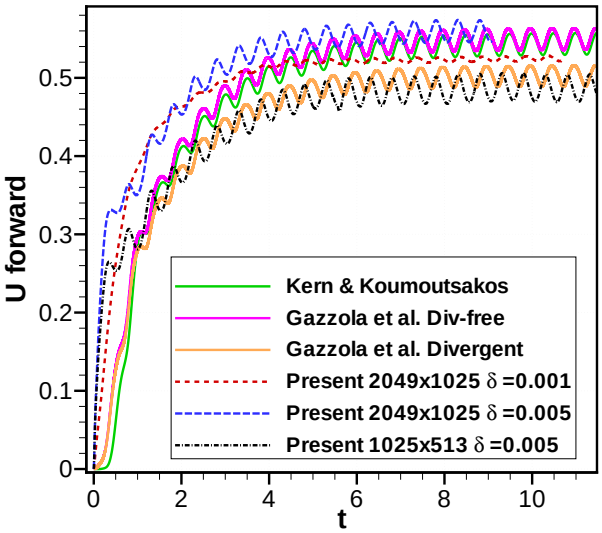

Figure 1: Anguilliform 2D swimmer's ($\lambda = f = 1$) forward velocity U. Solid lines indicate reference simulations performed by Kern and Koumoutsakos (green) [9] and Gazzola et al. (pink and brown) [14]. Dashed lines represent the results with the proposed algorithm.

4 APPLICATIONS AND RESULTS

Fish maneuvering law for tracking a fixed goal starting from rest is done by adding a constant curvature $k_{\text{offset}}(\theta_{\text{des}}, t)$ via Eq. (22) all along the fish's backbone $\xi \in [0, l_{\text{fish}}]$, to the primary propulsion mode, i.e., $k_3 = k(\xi, t) + k_{\text{offset}}$. However the change of the curvature must be gradually, i.e., $O(\Delta t)$. First a desired curvature k_{des} must be evaluated by the following relation,

$$k_{\text{des}}(\theta_{\text{des}}) = \begin{cases} -\text{sgn}(\theta_{\text{des}})\ k_{\max} & |\theta_{\text{des}}| \geq \theta_{\text{limit}} \\ -\text{sgn}(\theta_{\text{des}})\ k_{\max}\ (\frac{\theta_{\text{des}}}{\theta_{\text{limit}}})^2 & \text{else} \end{cases} \tag{21}$$

where *sgn* represents the sign function, i.e., $\text{sgn}(\theta_{\text{des}}) = \theta_{\text{des}}/|\theta_{\text{des}}|$. See Fig. (2) for a schematic representation of θ_{des}. In each time step according to the position and direction

of the head by considering the target a desired angle θ_{des} will be calculated. Then by using Eq. (21) a desired curvature k_{des} must be found. After that k_{offset} will be evaluated with the following relation,

$$k_{\text{offset}}^{n+1}(k_{\text{des}}) = \begin{cases} k_{\text{offset}}^{n} + \Delta k & k < k_{\text{desired}} \\ k_{\text{offset}}^{n} - \Delta k & \text{else} \end{cases} \tag{22}$$

k_{offset} will be added to the backbone curvature for rotation control, where $\Delta k = \Delta t\, \pi / T$. We are using $k_{\text{max}} = \pi$ which is equivalent to turning with a curvature adapted to a semicircle. As in Bergmann and Iollo [15] we are using $\theta_{\text{limit}} = \pi/4$. Time derivative of the curvature dk/dt is needed in Eq. (15) and can be calculated numerically. To show the performance of the proposed method a test case of food finding with the above rotation law is performed. The domain size is $(x, y) \in [0, 5l_{\text{fish}}] \times [0, 5l_{\text{fish}}]$, the resolution is set to 1025×1025, the penalization parameter $\eta = 10^{-3}$, filter parameter $\delta = 0.005$, tail beat frequency $f = 1$, wavelength $\lambda = 1$, kinematic viscosity $\nu = 1.4 \times 10^{-4}$, initial position of the head $(x_0, y_0) = (0.1L_x, 0.5L_y)$ and initial angle of the head $\theta_0 = 0$. Fig. 3 shows the snapshots of vorticity isolines obtained during a simulation of swimming fish for finding a food which is located at $(x_f, y_f) = (0.9L_x, 0.5L_y)$. At $t = 0$ the fish and the surrounding flow are in rest. After reaching the vicinity ($r_{\text{food}} = 0.5l_{\text{fish}}$) of the food the curvature of the backbone, given by Eq. (20), will tends to zero by multiplying it with the following function,

$$C(t) = \frac{t_f - t}{t_f - t_i} + \frac{1}{2\pi} \sin(2\pi \frac{t - t_i}{t_f - t_i}) \ , \ t \in [t_i, t_f] \tag{23}$$

with $t_i = t_{\text{reached}}$, $t_f = t_{\text{reached}} + T$ for gradually decreasing the curvature of the backbone during one period. See [17] for more details.

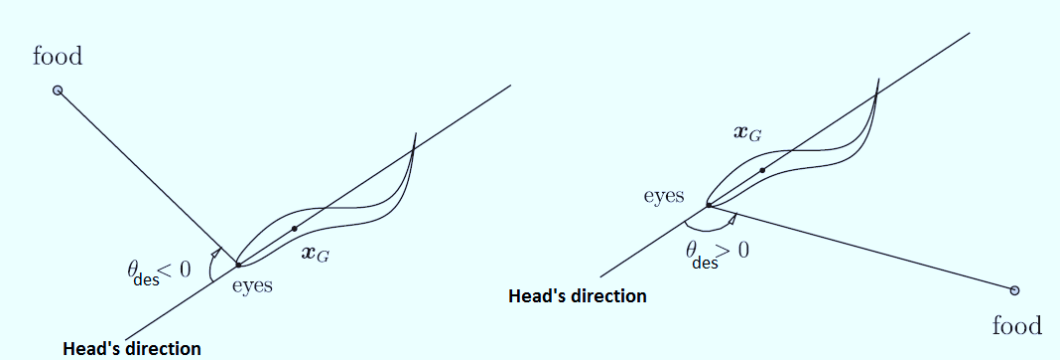

Figure 2: Schematic representation of desired angle for curvature control, $\theta_{\text{des}} = \theta_{\text{food}} - \theta_{\text{Head}}$ is the difference of the angles between head's direction and food's angle ($-\pi < \theta_{\text{des}} < \pi$), picture from Bergmann and Iollo [15] with a slight modification.

5 CONCLUSIONS

In this paper an efficient algorithm for simulation of deformable bodies interacting with two-dimensional incompressible flows is proposed. By using a uniform Cartesian grid a new fourth-order direct solver for the solution of the Poisson equation is presented. For introducing a deformable body in fluid flow, volume penalization method is applied to the solution of the Navier-Stokes equations as a forcing term. Even if penalization method is first-order in space, an important advantage of this method is that the evaluation of the hydrodynamic coefficients are straightforward. An efficient law for curvature control of an anguilliform swimmer looking for a food is proposed which is based on geometrically exact theory of nonlinear beam. Validation of the developed method shows the efficiency and expected accuracy of the algorithm for fish-like swimming control and also for a variety of fluid/solid interaction problems. Some guides for future developments is to use a high-order immersed boundary method, adding a multi-resolution analyses to the algorithm for grid adaptation, enhancement of rotation law, parallelization and extension to three dimensions. The code is developed in FORTRAN and is accessible for all [18].

Acknowledgment
We give our thanks to professor Boyer and colleagues for useful discussions, and sending their code describing Eel's backbone kinematics in forward gait.

REFERENCES

[1] P. Bontoux, B. Forestier and B. Roux, Analyse et optimisation d'une méthode de haute précision pour la résolution des équations de Navier-Stokes instationnaires. Journal de Mécanique Appliquée, 2, 3, 291-313, 1978.

[2] B. Roux, P. Bontoux, T. P. Loc and O. Daube, Optimisation of hermitian methods for Navier-Stokes equations in the vorticity and stream-function formulation. West Germany, September 9-15, 1979. (A81-36526 16-34) Berlin, Springer-Verlag, p. 450-468, 1980.

[3] J. C. Simo, A fnite strain beam formulation. The three-dimensional dynamic problem. Part I, Computer methods in applied mechanics and enginering, Vol. 49, 55-70, 1985.

[4] S. K. Lele, Compact finite difference schemes with spectral-like resolution. Journal of Computational Physics, Vol. 103, 16-42, 1992.

[5] H. Press, A. Teukolsky, T. Vetterling and P. Flannery, Numerical Recipes. Cambridge University Press, 1992.

[6] P. Orlandi, Fluid flow phenomena: A numerical toolkit. Springer, 2000.

[7] S. Abide and S. Viazzo, A 2D compact fourth-order projection decomposition method. Journal of Computational Physics, Vol. 206, 252-276, 2005.

[8] F. Boyer, M. Porez and W. Khalil, Macro-continuous computed torque algorithm for a three-dimensional Eel-like robot. IEEE Transactions on Robotics, Vol. 22, No. 4, 763-775, August 2006.

[9] S. Kern and P. Koumoutsakos, Simulations of optimized anguilliform swimming. Journal of Experimental Biology, Vol. 209, 4841-4857, 2006.

[10] M. El Rafei, M. Alamir, N. Marchand, M. Porez and F. Boyer, Multi-variable constrained control approach for a three-dimensional Eel-like robot. Published in IEEE/RSJ 2008 International Conference on Intelligent Robots and Systems, IROS, Nice, France, 2008.

[11] D. Kolomenskiy and K. Schneider. A Fourier spectral method for the Navier-Stokes equations with volume penalization for moving solid obstacles. Journal of Computational Physics, vol. 228, no. 16, 5687-5709, 2009.

[12] S. Laizet, E. Lamballais and J.C. Vassilicos. A numerical strategy to combine high-order schemes, complex geometry and parallel computing for high resolution DNS of fractal generated turbulence. Computers & Fluids, Vol. 39-3, pp 471-484, 2010.

[13] D. Rossinelli, M. Bergdorf, G. H. Cottet and P. Koumoutsakos, GPU accelerated simulations of bluff body flows using vortex particle methods. Journal of Computational Physics, Vol. 229, 3316-3333, 2010.

[14] M. Gazzola, P. Chatelain, W. M. van Rees and P. Koumoutsakos, Simulations of single and multiple swimmers with non-divergence free deforming geometries. Journal of Computational Physics, Vol. 230, 7093-7114, 2011.

[15] M. Bergmann and A. Iollo, Modeling and simulation of fish-like swimming. Journal of Computational Physics, Vol. 230, 329-348, 2011.

[16] A. Belkhiri, Modélisation dynamique de la locomotion compliante : Application au vol battant bio-inspiré de l'insecte. Thèse de doctorat, École nationale supérieure des mines de Nantes, 2013.

[17] S. A. Ghaffari, S. Viazzo, K. Schneider and P. Bontoux, Simulation of forced deformable bodies interacting with two-dimensional incompressible flows; Application to fish-like swimming. Preprint, Laboratoire M2P2-UMR 7340-CNRS, Centale Marseille, Aix-Marseille University, 2014, http://hal.archives-ouvertes.fr/hal-00967077.

[18] *The code is developped in FORTRAN and is accessible for all by sending a mail to*: ghaffari@L3m.univ-mrs.fr or s.amin.ghaffary@gmail.com

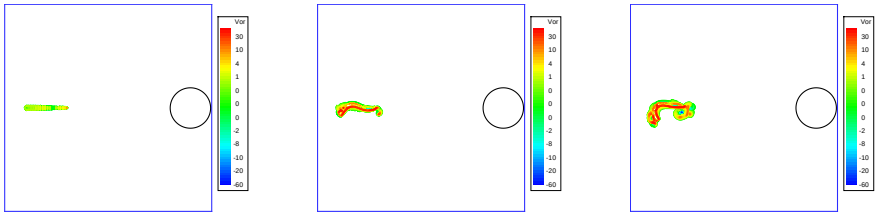

(a) $t = 0$ (b) $t = 1$ (c) $t = 2$

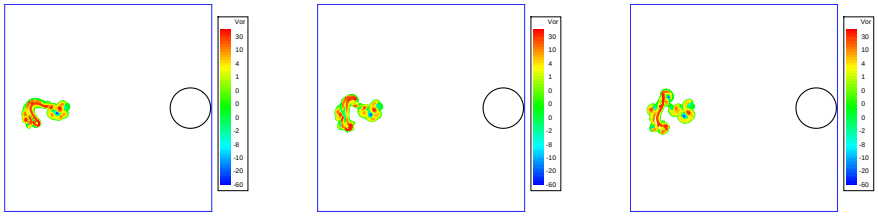

(d) $t = 2.3$ (e) $t = 2.6$ (f) $t = 3$

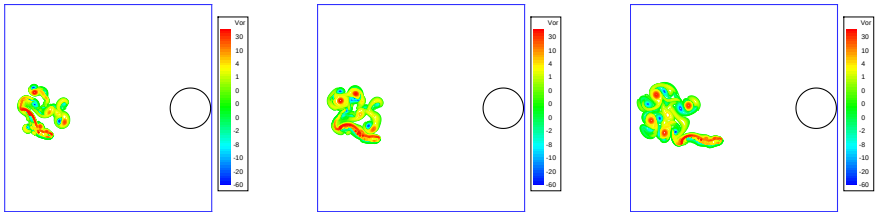

(g) $t = 4$ (h) $t = 5$ (i) $t = 7$

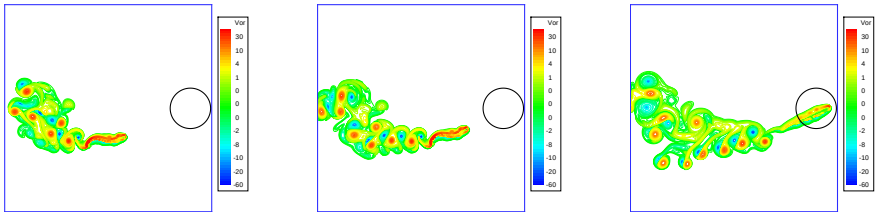

(j) $t = 9$ (k) $t = 11$ (l) $t = 15$

Figure 3: The snapshots of vorticity isolines obtained during a simulation of swimming fish for finding a food which is located at $(x_f, y_f) = (0.9L_x, 0.5L_y)$. At $t = 0$ the fish and the surrounding flow are in rest. After reaching the vicinity ($r = 0.5l_{\text{fish}}$) of the food the curvature of the backbone will tends to zero by Eq. (23). The domain of the solution is $(x, y) \in [0, 5l_{\text{fish}}] \times [0, 5l_{\text{fish}}]$, the resolution of the grid 1025×1025 and kinematic viscosity equal to $\nu = 1.4 \times 10^{-4}$.